lubricants

MDPI

Article

Assessing the Tribological Impact of 3D Printed Carbon-Reinforced ABS Composite Cylindrical Gears

Razvan George Ripeanu, Maria Tănase *, Alexandra Ileana Portoacă * and Alin Diniță *

Mechanical Engineering Department, Petroleum-Gas University of Ploiești, 100680 Ploiesti, Romania; rrapeanu@upg-ploiesti.ro

* Correspondence: maria.tanase@upg-ploiesti.ro (M.T.); alexandra.portoaca@upg-ploiesti.ro (A.I.P.); adinita@upg-ploiesti.ro (A.D.)

Abstract: The tribological performance of carbon-reinforced acrylonitrile butadiene styrene (ABS) composites is very important in determining their suitability for advanced engineering applications. This study employs response surface methodology (RSM) to evaluate the effects of printing temperature and post-processing annealing on the wear resistance and frictional properties of these composites. A central composite design is used to systematically explore the interaction between these two factors, enabling the development of predictive models for key tribological parameters. The results reveal that both the coefficient of friction (COF) and wear are affected by printing and annealing temperatures, although in a non-linear manner. Moderate printing temperatures and lower annealing temperatures were found to reduce friction and wear, with annealing temperature having a more pronounced effect on wear. To further optimize these responses, the desirability approach was applied for predicting the optimal conditions. The optimal combination of input parameters for minimizing both COF and wear was found to be a printing temperature of 256 °C and an annealing temperature of 126 °C. This research provides valuable insights for optimizing additive manufacturing processes of carbon-reinforced ABS composites, contributing to enhanced material durability in practical applications.

Keywords: 3D printing; ABS carbon reinforced; RSM; coefficient of friction; wear

Citation: Ripeanu, R.G.; Tănase, M.; Portoacă, A.I.; Diniță, A. Assessing the Tribological Impact of 3D Printed Carbon-Reinforced ABS Composite Cylindrical Gears. *Lubricants* **2024**, *12*, 376. https://doi.org/10.3390/lubricants12110376

Received: 4 October 2024
Revised: 29 October 2024
Accepted: 29 October 2024
Published: 30 October 2024

1. Introduction

Fundamental materials, such as PLA, have extensive baseline mechanical data [1] available for entry-level 3D printers. These data are valuable for both hobbyists and industrial end users. Different examinations of PLA [2] show how selecting optimal FDM parameters, such as a layer thickness of 0.2 mm and a print speed of 40 mm/s, can significantly enhance mechanical properties, setting the stage for more advanced studies.

Fiber reinforcement is a recurring theme in the literature [3], and it has been demonstrated that increasing carbon fiber content in composites boosts compressive strength by more than 30% compared to non-reinforced counterparts. There are many benefits [4] of integrating continuous carbon, glass, and Kevlar fibers in polymers, which substantially increase tensile strength to values exceeding 80 MPa [5]; short carbon fibers significantly enhance ABS's mechanical properties, improving impact resistance by around 25%.

The role of process parameters in determining material properties cannot be overstated, and it is necessary [6] to optimize the 3D printing parameters, such as layer thickness, to improve ABS performance. Different studies have emphasized achieving optimal results at a layer height of 0.15 mm and a printing temperature of 240 °C. In [7], numerical models are validated, showing that fine-tuning the build orientation and speed can reduce deformation. As demonstrated in [8], a 10% increase in infill density can improve ABS's wear resistance by 20%, which is crucial for friction-reducing applications. Another study [9] emphasized the importance of printing temperature, noting its significant impact on the mechanical integrity of ABS parts when set between 220 °C and 240 °C.

Annealing and other post-processing techniques are indispensable for enhancing 3D-printed materials. Studies by Arjun et al. [10] and Butt and Bhaskar [11] show that annealing at 80 °C for 2 h improves tensile strength by up to 15% and reduces anisotropy in thermoplastics; it has also been reported that annealing strengthens FDM 3D-printed ABS by enhancing its crystallinity and mechanical properties [12].

Tribological behavior, which involves wear and frictional characteristics, plays an important role in the performance of 3D-printed materials. One scientific study [8] highlights how specific infill densities of 60% can significantly improve wear resistance by up to 30%, which is an essential factor for components subjected to friction. The addition of 5% graphite as a lubricant in ABS improves wear resistance [13], reducing friction coefficients by as much as 0.1 units. FDM parameters combined with annealing improve both mechanical and tribological properties in PEEK [14], showcasing the benefits of comprehensive process understanding.

Advanced methodologies, like response surface methodology, have been employed by El Magri and Vaudreuil [15] and Mourya et al. [16] to systematically improve mechanical and tribological outcomes, showing the power of quantitative optimization techniques in material science. These authors used multiobjective optimization to specifically enhance the tribological characteristics of ABS and PLA polymers, optimizing them for reduced wear and increased durability.

Incorporating sustainable and bio-based materials introduces an environmental dimension to additive manufacturing. The use of plant fiber-based biocomposites [17] suggests sustainable alternatives in material formulation. Meanwhile, Pervaiz et al. [18] provided a comprehensive overview of current advancements and challenges with respect to fiber-reinforced plastic composites in 3D printing.

The use of machine learning to predict material properties [19] represents a significant leap forward. Analyses on carbon-reinforced ABS honeycomb structures highlights the potential of predictive modeling in optimizing design parameters for improved strength and application-specific performance.

In terms of mechanical properties optimization, different studies on annealing [20] and on using carbon and Kevlar fibers in composites [21] provide significant insights into maximizing the strength and flexibility of 3D-printed components. Further discussions on the anisotropic mechanical properties of FDM-printed ABS [22] highlight the need for design considerations in engineering applications.

Overall, the combination of fiber reinforcement, optimal printing parameters, and post-processing techniques like annealing is essential in producing 3D-printed parts with superior mechanical and tribological properties. This comprehensive research indicates a bright future for tailored additive manufacturing, addressing application-specific needs across a range of industries.

The novelty of this paper lies in its comprehensive approach to understanding and optimizing the tribological behavior of ABS–CF 3D printed gears for small industrial machines or drive systems that require force and precision, by focusing on the impact of both printing and annealing temperatures. The study uniquely employs a central composite design (CCD) and response surface methodology (RSM) to systematically analyze and optimize these parameters, revealing non-linear relationships between temperature settings and both coefficient of friction (COF) and wear. By identifying the optimal conditions for minimizing friction and wear, the research provides valuable insights that go beyond traditional methods, highlighting the importance of precise parameter control in 3D printing.

2. Materials and Methods

2.1. Experimental Design

The experiments were structured using a central composite design (CCD) within the framework of response surface methodology (RSM). This approach was employed to evaluate the interactions between the independent variables (in this case—printing temperature and annealing temperature), develop a mathematical model of the system,

and minimize the number of experimental runs [19]. The design enables the fitting of a second-order polynomial model and allows for the exploration of both linear and quadratic effects as well as interaction between the variables.

The first step consisted of defining the factor levels:

- Printing temperature (P): 250 °C (low) to 270 °C (high)
- Annealing temperature (A): 110 °C (low) to 130 °C (high)

The CCD was configured as follows:

- Factorial points: 2^2 factorial combinations of the low and high levels for each factor.
- Axial points: Axial points were added at $\pm\alpha$ ($\alpha = \sqrt{2}$, which is approximately 1.414, extending beyond the range of the factorial points to estimate curvature).
- Center points: Five replicates of the central condition were included to evaluate experimental error and provide an internal check for the adequacy of the model. The levels (low, center and high) for the considered printing parameters are presented in Table 1.

Table 1. Significant factors with their levels.

Factor	Levels		
	−1	**0**	**1**
Printing temperature (°C)	250	260	270
Annealing temperature (°C)	110	120	130

The axial points were calculated as:
For printing temperature:

$$\begin{aligned} P_{-\alpha} &= 260 - (270 - 260) \cdot \sqrt{2} = 246\ ^\circ\text{C} \\ P_{+\alpha} &= 260 + (270 - 260) \cdot \sqrt{2} = 274\ ^\circ\text{C} \end{aligned} \quad (1)$$

For annealing temperature:

$$\begin{aligned} A_{-\alpha} &= 120 - (130 - 120) \cdot \sqrt{2} = 106\ ^\circ\text{C} \\ A_{+\alpha} &= 120 + (130 - 120) \cdot \sqrt{2} = 134\ ^\circ\text{C} \end{aligned} \quad (2)$$

The experimental design matrix comprised 13 runs, including:

- Four factorial points at ($\pm$1, $\pm$1) (runs 1–4) representing the combinations of high and low levels of printing and annealing temperatures,
- Four axial points ($\pm\alpha$, 0) and (0, $\pm\alpha$) (runs 5–8) extending beyond the factorial range, allowing for the detection of curvature in the response surface,
- Five center points at the mid-level of each factor (runs 9–13), repeated to estimate the pure error, providing robustness to the model.

The experimental data (coefficient of friction, COF and wear, W) were then analyzed using analysis of variance (ANOVA) to determine the significance of the linear, quadratic and interaction effects of the factors on the response. A second order polynomial model was fitted to the data, represented as [15]:

$$Y = \beta_0 + \beta_1 P + \beta_2 A + \beta_{11} P^2 + \beta_{22} A^2 + \beta_{12} PA + \varepsilon \quad (3)$$

where Y is the predicted response (COF, W), β_0 is the intercept, β_1, β_2 are the linear coefficients, β_{11}, β_{22} are quadratic coefficients, β_{12} is the interaction coefficient, and ε is the experimental error.

The adequacy of the model was assessed by examining the R^2 value.

The response surfaces and contour plots were generated to visualize the effect of the independent variables on the response. The optimum conditions for printing and annealing temperatures were determined by minimizing the responses (both COF and W).

The statistical analysis was performed using the software Minitab version 19.

2.2. 3D Printing of Specimens

ABS–CF filaments were supplied by Kimya (Nantes, France) and belong to the styrenic polymer family. Acrylonitrile–butadiene–styrene–carbon (ABS carbon) is a mixture of ABS and carbon fibers in 15% carbon proportion, which give the filament improved rigidity compared to a standard ABS. The filament used has a 1.75 mm diameter, a density of 1.048 g/cm^3, a glass transition temperature of 108 °C and a melt flow index of 17.4 g/10 min. Mechanical properties such as tensile modulus (3396 MPa), tensile strength (36.7 MPa), Charpy impact resistance (18 kJ/m^2) are included in the technical specification of the filament.

Using the printing temperatures presented in Table 2 (the low and high value were selected considering the provider's suggested range of extrusion temperature), the specimens in the form of discs with 15 mm radius (Figure 1) were 3D printed with a Raise E2 3D printer (Raise3D, Shanghai, China) and using a ruby nozzle with a 0.4 mm diameter, due to the premature wear risk caused by the carbon fiber in the filament material. Afterwards, they were subjected to post-processing heat treatment for 2 h in an oven, at different annealing temperatures, according to the experimental design presented in Table 2.

Table 2. Experimental design matrix.

Exp. No.	Printing Temperature, *P* (°C)	Annealing Temperature, *A* (°C)
1	250	110
2	270	110
3	250	130
4	270	130
5	246	120
6	274	120
7	260	106
8	260	134
9	260	120
10	260	120
11	260	120
12	260	120
13	260	120

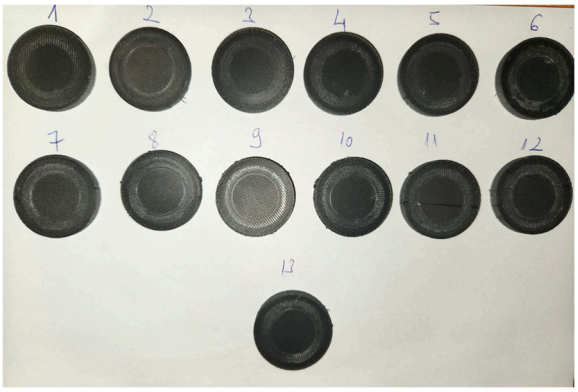

Figure 1. 3D printed specimens after tribological testing.

The constant printing parameters were: layer thickness 0.2 mm, 2 shells and 4 bottom and top layers and a filling percentage of 50% because, in this case, the tribological properties investigated were more susceptible to the quality of the surface rather than the interior of the printed samples, and the variable factors were referring to the temperatures of extrusion and annealing.

2.3. Tribological Testing

The wear tests were designed based on the torque transmission of a cylindrical gear assembly, with the geometrical characteristics outlined in Table 3. The coefficients of friction were measured using a CSM Instruments THT pin-on-disc tribometer (CSM Instruments, Freiburg in Breisgau, Germany) (as seen in Figure 2).

Table 3. Geometrical specification of the gear application.

Geometric Parameters	Values
Number of teeth	12
Module	4.5 mm
Pressure angle	20°
Type of gearing	External
Tip diameter	63 mm
Pitch diameter	54 mm
Root diameter	42.75 mm
Base diameter	50.7434 mm
Addendum	4.5 mm
Dedendum	5.625 mm
Width	8.5 mm
Shaft mounting diameter	10 mm

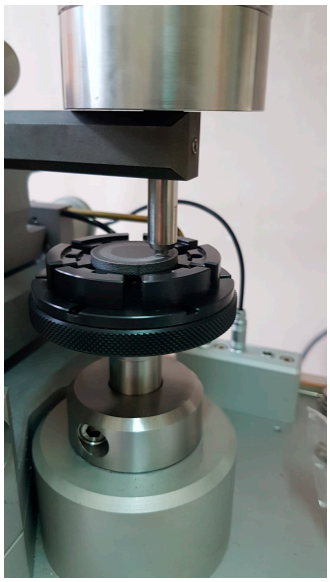

Figure 2. Experimental device used to determine the sliding coefficient of friction.

The friction pair consisted of a 20 mm diameter disc sample of ABS–CF material and the 4 mm cub from the material AISI4130 alloy steel, referring to an assembly formed by two gears made from the considered materials.

Furthermore, the tribological tests were performed under the following conditions: a normal load of 10 N (which applies a contact pressure comparable to the Hertzian pressure in the gears of 0.625 MPa, considering a nominal torque generated by a 370 W electric motor operating at 575 RPM), a friction distance of 250 m, and a linear speed of 0.60 m/s. All tests were performed at room temperature (23 °C) in ambient air with 54% relative humidity. The coefficient of friction (μ) was calculated as the ratio of the tangential friction force to the normal force and the cumulative linear wear was calculated as the difference between maximal and minimal penetration, excluding the peaks [23,24]. For each combination of printing parameters, three friction pairs, class 4th, were tested. Continuous measurements were recorded, with an acquisition rate of 9.5 Hz, during the tests to determine the coefficient of friction and the cumulative linear wear.

3. Results and Discussion

3.1. Experimental Results Regarding the Tribological Properties of ABS–CF 3D Printed Samples

Table 4 and Figure 3 provide a comprehensive overview of the data collected during the experimental investigation, detailing the measured outcomes and variables across a range of controlled conditions, allowing for in-depth analysis and interpretation of the experimental results.

Table 4. Experimental results according to DOE.

Exp. No.	Factor		Response			
			COF		Wear, µm	
	Printing Temperature, *P* (°C)	Annealing Temperature, *A* (°C)	Mean Value	Standard Deviation	Mean Value	Standard Deviation
1	250	110	0.25	0.0049	129.479	54.961
2	270	110	0.281	0.0289	148.568	30.053
3	250	130	0.308	0.0076	59.823	17.834
4	270	130	0.319	0.0124	91.930	23.437
5	246	120	0.217	0.0235	98.542	27.552
6	274	120	0.293	0.0217	88.201	2.418
7	260	106	0.276	0.0030	58.986	15.314
8	260	134	0.228	0.0163	66.832	13.683
9	260	120	0.229	0.0113	66.803	32.065
10	260	120	0.246	0.0128	31.044	19.643
11	260	120	0.218	0.0122	98.547	43.112
12	260	120	0.236	0.0145	130.856	41.153
13	260	120	0.221	0.0116	126.393	38.179

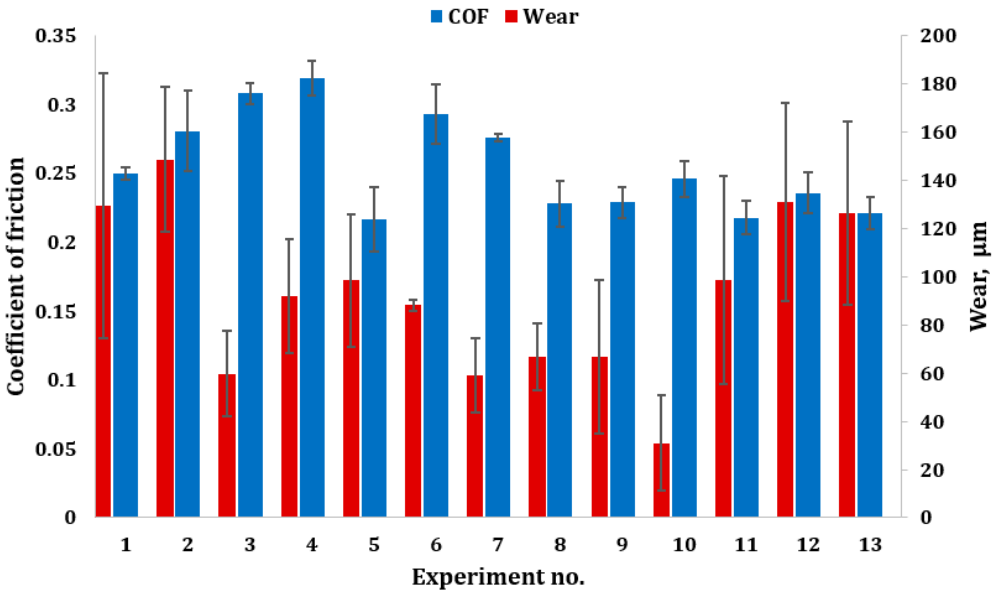

Figure 3. Experimental results for coefficient of friction and wear.

For the considered ranges of input parameters, the lowest value of COF is 0.217, the highest is 0.319 and the average recorded was 21.9% higher than the COF mentioned in reference [25]. For wear, the lowest value observed is 31.044 µm, the highest is 148.568 µm and the average was 21.67% lower than the ABS printed material studied in [25], which suggests a better tribological performance because of the self-lubricating properties added by the carbon fibers in the material.

It can be observed that, at lower printing temperatures, the COF tends to be lower, with the minimum COF of 0.217 recorded at 246 °C. Conversely, higher printing temperatures

(e.g., 270 °C) are associated with higher COF values. Increasing the annealing temperature generally leads to an increase in COF, except for specific combinations where the effect might differ.

The wear values show more variation with changes in both printing and annealing temperatures. For example, at a printing temperature of 260 °C and an annealing temperature of 120 °C, wear values range from 31.044 µm to 130.856 µm. This suggests that the optimal condition for reducing wear might involve specific settings of printing and annealing temperatures.

In published studies, researchers have analyzed the influences of other printing parameters such as layer thickness, nozzle temperature, line width, printing speed [16], material deposition layer thickness, infill angle, infill pattern and orientation of deposition [25], and infill density [8] on the wear characteristics of 3D printed ABS parts.

The standard deviation values for COF range from 0.0030 to 0.0289. The lowest standard deviation was recorded for experiment No. 7, with the highest for experiment No. 2. When analyzing the wear data, it can be seen that standard deviation shows greater variation, ranging from 2.418 to 54.961. For example, in experiment No. 1, the high standard deviation (54.961) suggests significant variability in wear. In contrast, a low standard deviation (e.g., 2.418 for experiment No. 6) indicates that the wear was consistent across the replicates for that experimental condition.

The presence of large error bars, particularly in wear measurements, emphasizes the need for careful control over printing and annealing parameters. In case of ABS carbon gears, reducing fluctuations in wear would ensure a more predictable and extended lifespan in applications like automotive systems or industrial machinery, where mechanical components are subject to high loads and continuous movement. Moreover, the consistent COF observed at specific temperature ranges suggests that ABS carbon gears produced under those conditions could provide reliable frictional performance. This is particularly beneficial in applications where gears are in constant motion and require steady contact with other components. A predictable COF helps ensure smooth gear operation, reducing the risk of slippage or mechanical failure in systems that rely on precision movements, such as robotics or conveyor systems.

3.2. ANOVA Analysis

The influence of printing parameters (*P* and *A*) on multiple response variables was evaluated using analysis of variance (ANOVA). To assess model performance, ANOVA was conducted on the results of a full quadratic model, with R_2 values calculated for evaluation.

The Pareto charts illustrate the main and interaction effects derived from the ANOVA, offering the added benefit of identifying the standardized effects of various linear, quadratic, and interaction terms of printing and annealing temperature compared to the reference threshold of 2.306 (as shown in Figure 4). Effects surpassing this threshold are deemed significant within the model.

In the case of coefficient of friction, the Pareto chart in Figure 4a shows that the interaction between printing and annealing temperatures (AB) has the most significant effect. The quadratic terms (AA and BB) also have notable effects, although slightly less impactful than the interaction term. Factor A (printing temperature) has a minimal effect, while factor B (annealing temperature) is less impactful compared to the interaction effects.

For wear, the quadratic term of annealing temperature (BB) is the most significant factor, while the main effects of annealing temperature (B) and printing temperature (A), as well as the quadratic term (AA), are less significant. The interaction between printing and annealing temperatures (AB) has the least effect on wear.

For better understanding of the effect of input variables, main effect plots (Figure 5) were drawn.

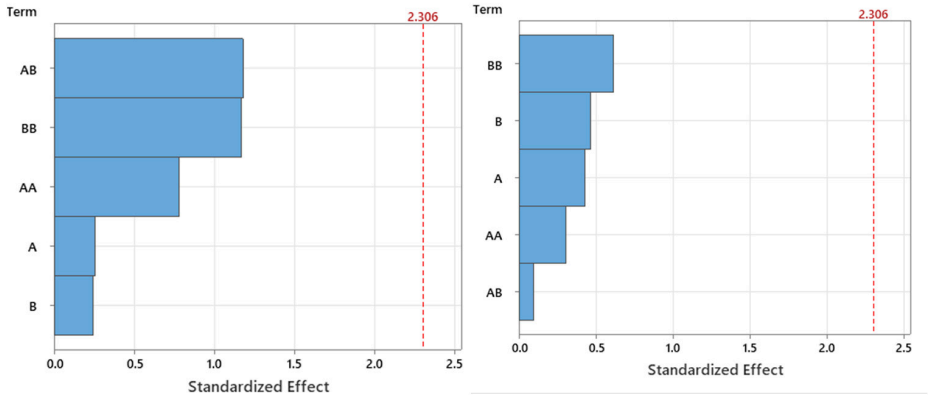

Figure 4. Pareto charts of the standardized effects of (**a**) coefficient of friction, (**b**) wear (factors: A—printing temperature, B—annealing temperature).

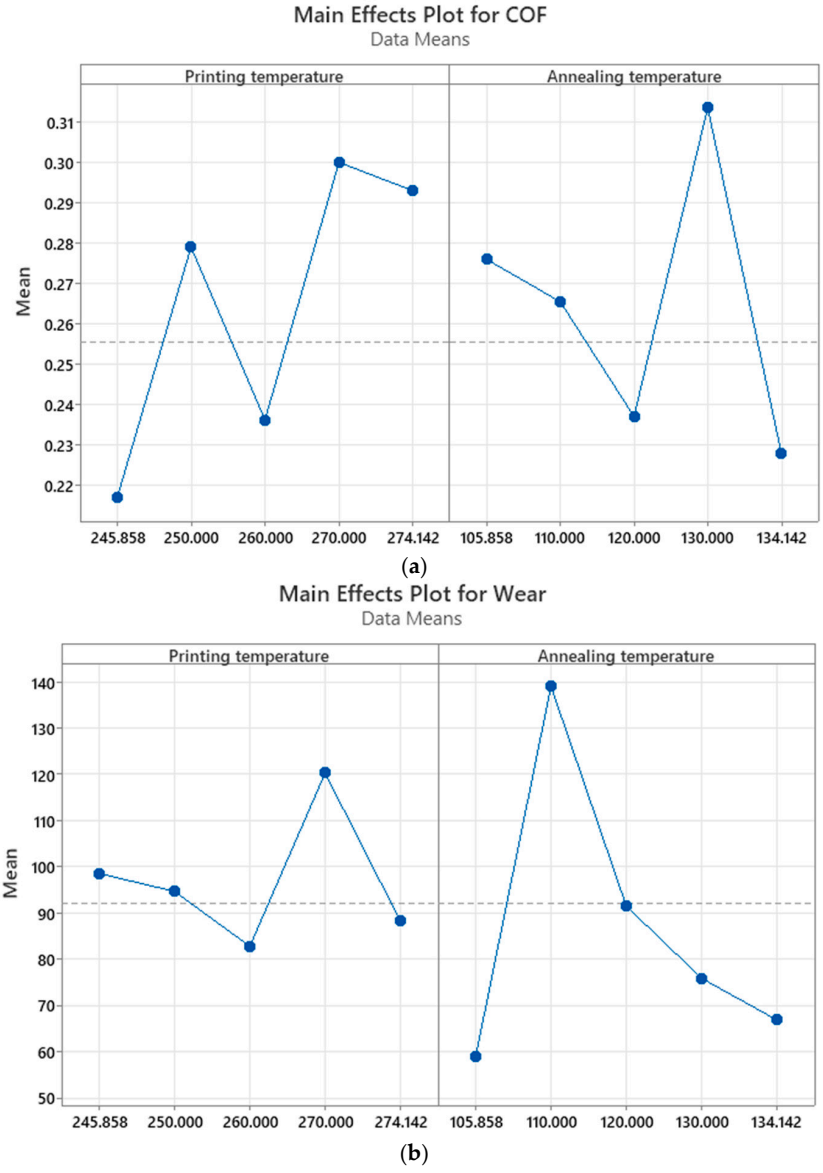

Figure 5. Main effects plots for (**a**) coefficient of friction, (**b**) wear (printing temperature and annealing temperature unit—°C).

In the plot in Figure 5a, the COF shows a distinct variation with printing temperature. The COF increases steadily, peaking around 270 °C, after which it declines slightly. This pattern indicates that printing temperature significantly impacts the frictional behavior, with higher temperatures leading to increased friction, although this effect begins to stabilize beyond a certain point. When considering annealing temperature, the COF generally decreases as the temperature rises (except for the temperature of 130 °C where the highest COF was obtained). The lowest COF is observed at maximum annealing temperature (134 °C), suggesting that higher annealing temperatures tend to reduce friction.

In the plot in Figure 5b, the relationship between wear and the temperature is also apparent.

For printing temperature, wear decreases slightly from 246 °C to 260 °C then increases sharply as the temperature rises, peaking at 270 °C, like the COF plot. After this point, the wear decreases slightly at the highest temperature. This pattern indicates that wear increases with higher printing temperatures, but beyond a certain point, it begins to drop.

Wear increases with printing temperature, peaking around 270 °C, similar to the COF, before dropping at higher temperatures. This implies that printing temperature significantly influences wear, with higher values leading to greater wear, up to a threshold. Regarding annealing temperature, wear reaches its highest point at around 120 °C, but then drops sharply as the temperature approaches 130 °C. This pattern reflects a non-linear relationship, where wear increases with annealing temperature until a certain point, after which it decreases. For annealing temperature, wear shows a non-linear trend. The wear increases from the annealing temperature of 106 °C, reaching a maximum at 110 °C, and then decreases significantly as the temperature increases to 134 °C. This suggests that moderate annealing temperatures contribute to higher wear, but at higher temperatures, wear decreases sharply.

A previous study [16] similarly reports that wear decreases significantly with increasing nozzle temperature, followed by a slight increase. The pattern in both studies suggests that moderate temperatures contribute to lower wear, but beyond a certain threshold, wear increases.

Regarding COF, in the previous study [16], a similar pattern is observed, where the COF initially increases with nozzle temperature and then decreases at higher temperatures.

Overall, both studies highlight the non-linear relationship between temperature and both COF and wear, with peak points beyond which performance begins to deteriorate.

The regression models for the selected responses were developed using response surface methodology (RSM). As shown in Table 5, all regression models demonstrate a high value of coefficient of determination (R^2) for each model, supporting their predictive accuracy and proving the utility of the study for specialists in the industry.

Table 5. RSM predictive regression models.

Response	RSM Model	R^2
COF	$COF = -0.0053\ P + 0.0109\ A + 0.000054\ P^2 + 0.000146\ A^2 - 0.000176\ PA$	98.9%
W	$W = -10.0\ P + 23.6\ A + 0.0239\ P^2 - 0.087\ A^2 - 0.016\ PA$	90.3%

Based on the RSM, predictive regression models represented the surface and contours of plots in Figure 6 and Figure 7, respectively, to better understand the interaction between the investigated parameters.

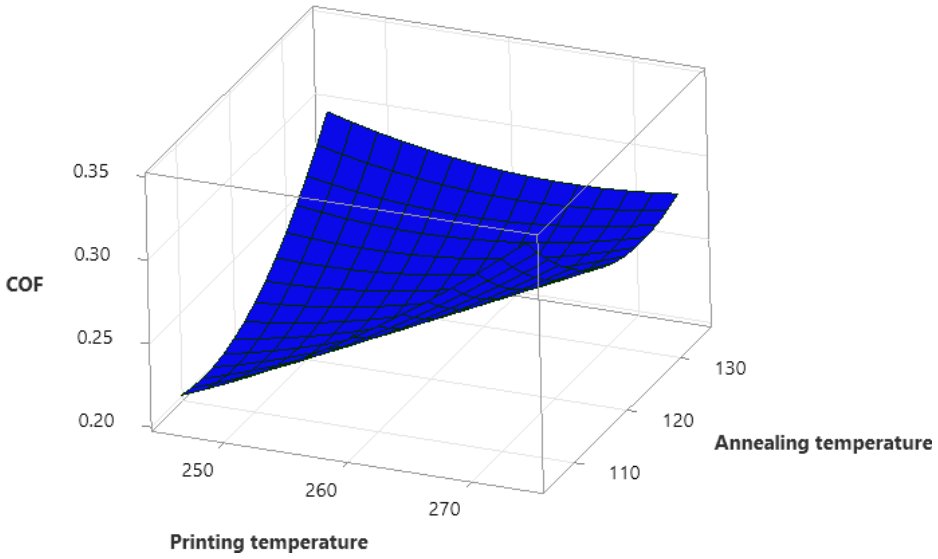

(**a**)

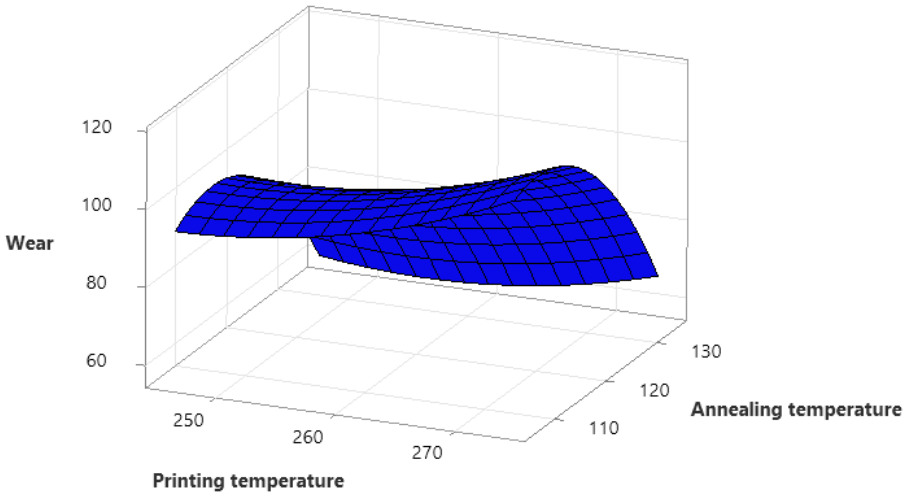

(**b**)

Figure 6. Surface plots for (**a**) coefficient of friction, (**b**) wear (printing temperature and annealing temperature unit—°C, wear unit—μm).

The graph in Figure 6a reveals that the COF increases as the printing temperature rises, with a more pronounced effect at higher annealing temperatures. In contrast, at lower printing temperatures, the COF remains relatively low. This surface plot indicates that both printing and annealing temperatures play a significant role in influencing COF, with the most notable interaction occurring when both parameters are elevated. The data in Figure 6b shows that wear remains stable across a wide range of printing temperatures. However, there is a slight increase in wear at higher printing temperatures, while mid to high annealing temperatures lead to a leveling off or even a slight reduction in wear at certain temperature combinations.

The contour plot in Figure 7a shows that COF values increase significantly, reaching above 0.30 (dark purple) at higher printing (~270 °C) and annealing (~130 °C) temperatures. Intermediate printing temperatures (~255–265 °C) correspond to moderate COF values, ranging from 0.24 to 0.28, represented by yellow to light purple colors. This plot shows that both printing and annealing temperatures contribute to an increase in COF, with distinct "hotspots" of high COF values forming at elevated temperatures for both parameters.

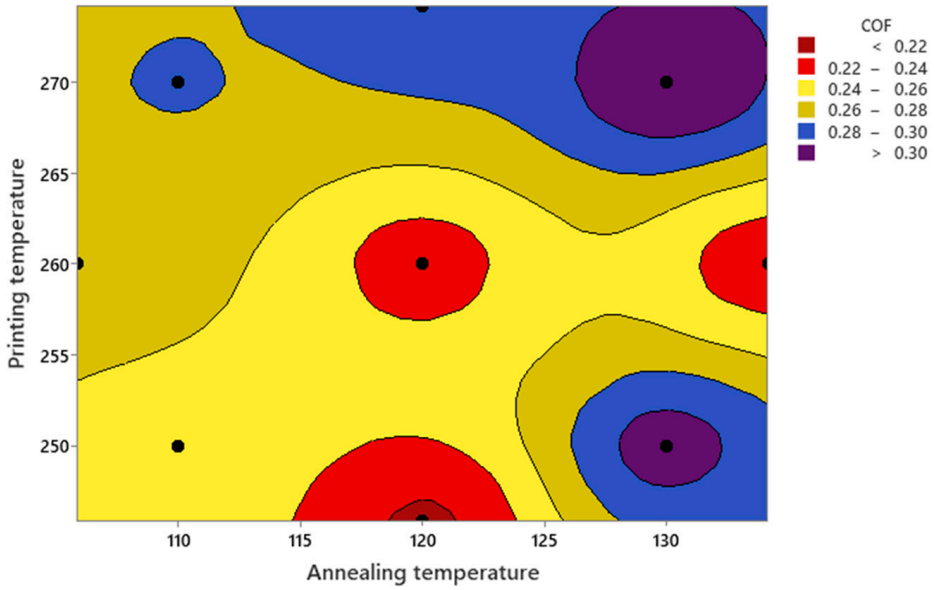

(**a**)

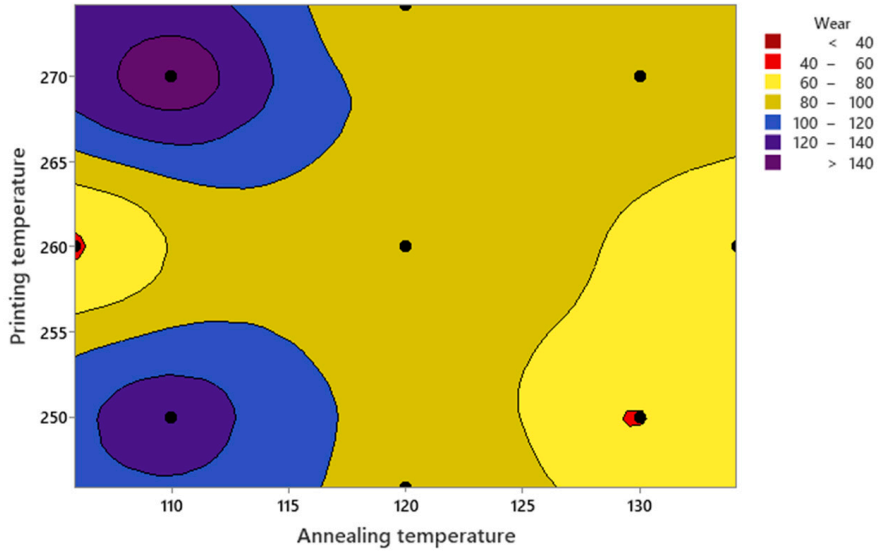

(**b**)

Figure 7. Contour plots for (**a**) coefficient of friction, (**b**) wear (printing temperature and annealing temperature unit—°C, wear unit—μm).

In the second contour plot (Figure 7b), it can be observed that lower wear values, below 40 μm (dark red), are observed in regions where the printing temperature is moderate (~255 °C) and the annealing temperature falls between 120–125 °C. The highest wear values, exceeding 140 μm (purple regions), are more sporadically distributed, with the most significant wear occurring at a combination of high printing temperature (~270 °C) and low annealing temperature (~110 °C). In general, moderate wear values, ranging from 80 to 100 μm, dominate much of the parameter space, indicating that wear does not fluctuate as much as COF. However, specific combinations of printing and annealing temperatures can lead to high or low wear, signaling opportunities for optimizing the process to reduce material degradation.

The interaction plots in Figure 8 are used to illustrate how changes in the printing and annealing temperatures influence the two responses variables (coefficient of friction (COF) and wear) simultaneously.

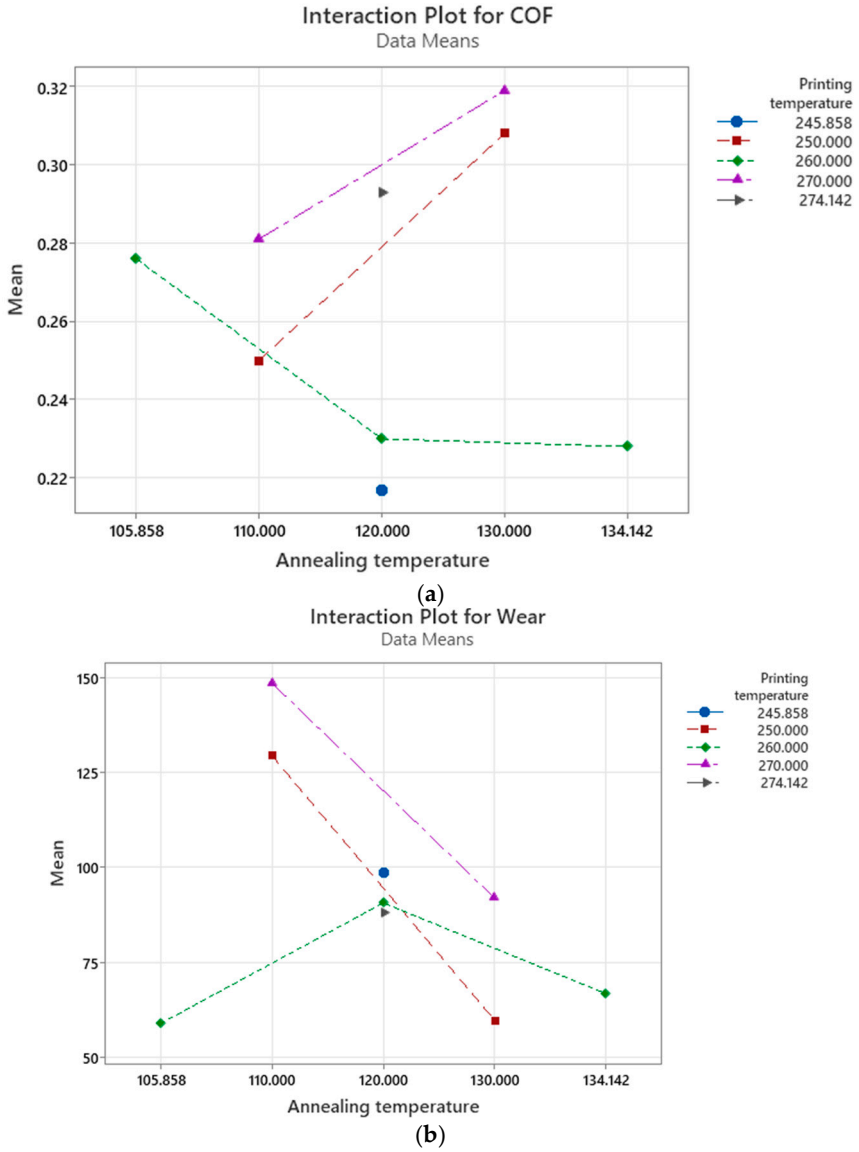

Figure 8. Interaction plots for (**a**) coefficient of friction, (**b**) wear (printing temperature and annealing temperature unit—°C).

When analyzing the first plot (Figure 8a), an interaction between printing and annealing temperatures is evident, as the lines do not run parallel, indicating that both factors influence the COF. At lower annealing temperatures (~105 °C), COF tends to decrease as the printing temperature increases, particularly for lower printing temperatures (as shown by the green and red lines). In contrast, at higher annealing temperatures (~130 °C), COF increases more sharply, especially at higher printing temperatures (seen in the purple and pink lines). This suggests that the largest increases in COF occur when both printing and annealing temperatures are high, indicating a strong interaction between the two parameters at these levels.

The plot in Figure 8b shows that, while the interaction effects for wear are less pronounced compared to COF, they are still present, as the lines are not perfectly parallel. At low annealing temperatures (~105 °C), wear decreases as printing temperature rises, especially for lower printing temperatures. However, at higher annealing temperatures (~130 °C), wear generally increases, particularly when the printing temperature is around 270 °C (represented by the purple line). Overall, wear tends to decrease with annealing temperature.

3.3. Multi-Response Optimization

The process parameters (printing and annealing temperature) are optimized for the coefficient of friction and wear, using the composite desirability function. For each response, the criteria for the optimization set are similar; namely, the objective is to minimize both coefficient of friction and wear of the ABS–CF 3D printed samples (as seen in Table 6). The multi-response optimization plot obtained using Minitab 19 software is shown in Figure 9 and it allows us to establish the following optimal settings to minimize both coefficient of friction and wear: 256 °C printing temperature and 126 °C annealing temperature.

Table 6. Optimization goals.

Response	Goal	Lower	Target	Upper	Weight	Importance
Wear	Minimum		31.0442	148.568	0.5	1
COF	Minimum		0.2170	0.319	0.5	1

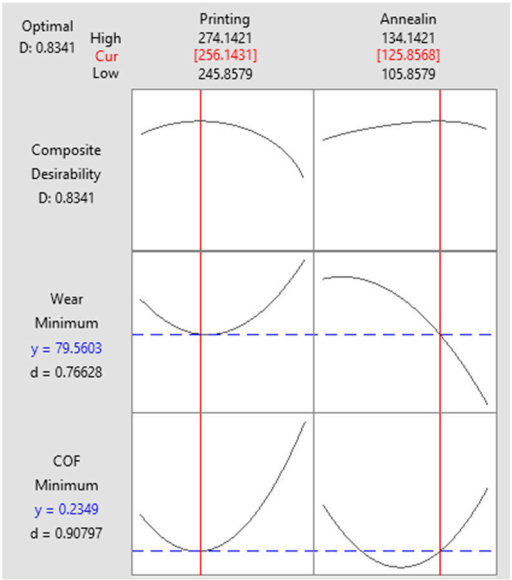

Figure 9. Optimization plot.

4. Conclusions

The aim of the present study was to study the impacts of two parameters, printing temperature and annealing temperature, on the tribological behavior of ABS–CF 3D printed gears. To evaluate the importance of each parameter while reducing the number of experiments, a central composite design (CCD) approach was employed. The statistical significance of each parameter was assessed using analysis of variance (ANOVA). Results indicate that both coefficient of friction and wear are influenced by printing and annealing temperatures, although the effects are non-linear. Moderate printing temperatures and lower annealing temperatures may help minimize friction and wear, with annealing temperature showing a more pronounced effect on wear.

Subsequently, response surface methodology (RSM) was applied to determine the regression models and to optimize the responses based on the input factors, thereby determining the optimal levels for printing temperature and annealing temperature, leading to minimum values for both coefficient of friction and wear. According to the RSM analysis, the optimal settings to minimize all output responses are a printing temperature of 256 °C and an annealing temperature of 126 °C.

Therefore, the investigation performed shows that adjusting the printing and annealing temperatures has a significant impact on both COF and wear, with lower printing

temperatures generally leading to lower COF but not consistently to lower wear. Careful selection of both parameters is needed to optimize the tribological properties of the material.

Future research could focus on exploring additional process parameters beyond printing and annealing temperatures, such as printing speed, infill density, and cooling rate, to better understand their influence on the tribological behavior of ABS–CF 3D printed parts. Long-term wear behavior under different operational conditions, such as changes in temperature and humidity, should also be studied to assess the durability and performance of ABS–CF parts over extended periods. In addition, exploring correlations between tribological properties and mechanical characteristics like tensile strength could provide more comprehensive insights for material optimization.

Author Contributions: Conceptualization, A.I.P., M.T. and A.D.; methodology, M.T., A.I.P. and R.G.R.; validation, R.G.R.; formal analysis, R.G.R.; investigation, A.I.P., M.T., A.D. and R.G.R.; resources, M.T., A.I.P., A.D. and R.G.R.; writing—original draft preparation, A.I.P. and M.T.; writing—review and editing, A.I.P., A.D., R.G.R. and M.T.; visualization A.I.P., R.G.R., A.D. and M.T.; supervision, R.G.R. All authors have read and agreed to the published version of the manuscript.

Funding: This research received no external funding.

Institutional Review Board Statement: Not applicable.

Informed Consent Statement: Not applicable.

Data Availability Statement: The original contributions presented in the study are included in the article, further inquiries can be directed to the corresponding authors.

Conflicts of Interest: The authors declare no conflicts of interest.

References

1. Letcher, T.; Waytashek, M. Material Property Testing of 3D-Printed Specimen in PLA on an Entry-Level 3D Printer. In *Advanced Manufacturing, Proceedings of the ASME International Mechanical Engineering Congress and Exposition, Montreal, QC, Canada, 14–20 November 2014*; American Society of Mechanical Engineers: Montreal, QC, Canada, 2014; Volume 2A, p. V02AT02A014.
2. Chacón, J.M.; Caminero, M.A.; García-Plaza, E.; Núñez, P.J. Additive Manufacturing of PLA Structures Using Fused Deposition Modelling: Effect of Process Parameters on Mechanical Properties and Their Optimal Selection. *Mater. Des.* **2017**, *124*, 143–157. [CrossRef]
3. Adeniran, O.; Cong, W.; Bediako, E.; Aladesanmi, V. Additive Manufacturing of Carbon Fiber Reinforced Plastic Composites: The Effect of Fiber Content on Compressive Properties. *J. Compos. Sci.* **2021**, *5*, 325. [CrossRef]
4. Dickson, A.N.; Barry, J.N.; McDonnell, K.A.; Dowling, D.P. Fabrication of Continuous Carbon, Glass and Kevlar Fibre Reinforced Polymer Composites Using Additive Manufacturing. *Addit. Manuf.* **2017**, *16*, 146–152. [CrossRef]
5. Lobov, E.; Dobrydneva, A.; Vindokurov, I.; Tashkinov, M. Effect of Short Carbon Fiber Reinforcement on Mechanical Properties of 3D-Printed Acrylonitrile Butadiene Styrene. *Polymers* **2023**, *15*, 2011. [CrossRef] [PubMed]
6. Ahmad, M.N.; Yahya, A. Effects of 3D Printing Parameters on Mechanical Properties of ABS Samples. *Designs* **2023**, *7*, 136. [CrossRef]
7. Al Rashid, A.; Koç, M. Experimental Validation of Numerical Model for Thermomechanical Performance of Material Extrusion Additive Manufacturing Process: Effect of Process Parameters. *Polymers* **2022**, *14*, 3482. [CrossRef]
8. Akıncıoğlu, G.; Şirin, E.; Aslan, E. Tribological Characteristics of ABS Structures with Different Infill Densities Tested by Pin-on-Disc. *Proc. Inst. Mech. Eng. Part J J. Eng. Tribol.* **2023**, *237*, 1224–1234. [CrossRef]
9. Ulkir, O.; Ertugrul, I.; Ersoy, S.; Yağımlı, B. The Effects of Printing Temperature on the Mechanical Properties of 3D-Printed Acrylonitrile Butadiene Styrene. *Appl. Sci.* **2024**, *14*, 3376. [CrossRef]
10. Arjun, P.; Bidhun, V.K.; Lenin, U.K.; Amritha, V.P.; Pazhamannil, R.V.; Govindan, P. Effects of Process Parameters and Annealing on the Tensile Strength of 3D Printed Carbon Fiber Reinforced Polylactic Acid. *Mater. Today Proc.* **2022**, *62*, 7379–7384. [CrossRef]
11. Butt, J.; Bhaskar, R. Investigating the Effects of Annealing on the Mechanical Properties of FFF-Printed Thermoplastics. *JMMP* **2020**, *4*, 38. [CrossRef]
12. Seok, W.; Jeon, E.; Kim, Y. Effects of Annealing for Strength Enhancement of FDM 3D-Printed ABS Reinforced with Recycled Carbon Fiber. *Polymers* **2023**, *15*, 3110. [CrossRef] [PubMed]
13. Dawoud, M.; Taha, I.; Ebeid, S.J. Effect of processing parameters and graphite content on the tribological behaviour of 3D printed acrylonitrile butadiene styrene: Einfluss von Prozessparametern und Graphitgehalt auf das tribologische Verhalten von 3D-Druck Acrylnitril-Butadien-Styrol Bauteilen. *Mater. Werkst* **2015**, *46*, 1185–1195. [CrossRef]
14. He, Y.; Shen, M.; Wang, Q.; Wang, T.; Pei, X. Effects of FDM Parameters and Annealing on the Mechanical and Tribological Properties of PEEK. *Compos. Struct.* **2023**, *313*, 116901. [CrossRef]

15. El Magri, A.; Vaudreuil, S. Optimizing the Mechanical Properties of 3D-Printed PLA-Graphene Composite Using Response Surface Methodology. *Arch. Mater. Sci. Eng.* **2021**, *112*, 13–22. [CrossRef]
16. Mourya, V.; Bhore, S.P.; Wandale, P.G. Multiobjective Optimization of Tribological Characteristics of 3D Printed Texture Surfaces for ABS and PLA Polymers. *J. Thermoplast. Compos. Mater.* **2024**, *37*, 772–799. [CrossRef]
17. Ramesh, M.; Palanikumar, K.; Reddy, K.H. Plant Fibre Based Bio-Composites: Sustainable and Renewable Green Materials. *Renew. Sustain. Energy Rev.* **2017**, *79*, 558–584. [CrossRef]
18. Pervaiz, S.; Qureshi, T.A.; Kashwani, G.; Kannan, S. 3D Printing of Fiber-Reinforced Plastic Composites Using Fused Deposition Modeling: A Status Review. *Materials* **2021**, *14*, 4520. [CrossRef]
19. Ranaiefar, M.; Singh, M.; Halbig, M.C. Additively Manufactured Carbon-Reinforced ABS Honeycomb Composite Structures and Property Prediction by Machine Learning. *Molecules* **2024**, *29*, 2736. [CrossRef]
20. Valvez, S.; Reis, P.N.B.; Ferreira, J.A.M. Effect of Annealing Treatment on Mechanical Properties of 3D-Printed Composites. *J. Mater. Res. Technol.* **2023**, *23*, 2101–2115. [CrossRef]
21. Wang, K.; Li, S.; Rao, Y.; Wu, Y.; Peng, Y.; Yao, S.; Zhang, H.; Ahzi, S. Flexure Behaviors of ABS-Based Composites Containing Carbon and Kevlar Fibers by Material Extrusion 3D Printing. *Polymers* **2019**, *11*, 1878. [CrossRef] [PubMed]
22. Ziemian, C.; Sharma, M.; Ziemi, S. Anisotropic Mechanical Properties of ABS Parts Fabricated by Fused Deposition Modelling. In *Mechanical Engineering*; Gokcek, M., Ed.; InTech: Incheon, Republic of Korea, 2012; ISBN 978-953-51-0505-3.
23. Portoaca, A.-I.; Ripeanu, G.-R.; Nae, I.; Tanase, M. The Influence of 3D Printing Parameters and Heat Treatment on Tribological Behavior. *Acta Tech. Napoc.* **2023**, *66*, 537–546.
24. Portoacă, A.I.; Ripeanu, R.G.; Diniță, A.; Tănase, M. Optimization of 3D Printing Parameters for Enhanced Surface Quality and Wear Resistance. *Polymers* **2023**, *15*, 3419. [CrossRef] [PubMed]
25. Roy, R.; Mukhopadhyay, A. Tribological Studies of 3D Printed ABS and PLA Plastic Parts. *Mater. Today Proc.* **2021**, *41*, 856–862. [CrossRef]